▸ *10.2.3 Splitting Diagrams*

Having discussed some of the requirements for transitions between energy states to occur, we now turn to an examination of what energy states are actually possible for transition metal ions in complexes. In Section 10.2.1 we discussed the number of states into which each free-ion term splits for an ion in a ligand field. We also need to understand how the energy separations between states depend on the identity of ligands through the value of $10Dq$.

Splittings for d^1, d^9, and High-Spin d^4 and d^6

The d^1 case, without electron repulsion, is simplest to treat because there is a one-to-one correspondence between electron configurations and states. The t_{2g}^1 configuration in O_h gives rise to a $^2T_{2g}$ state of energy, $-4Dq$. Promotion of the electron gives the e_g^1 configuration corresponding to the excited ^2E_g state of energy, $+6Dq$.

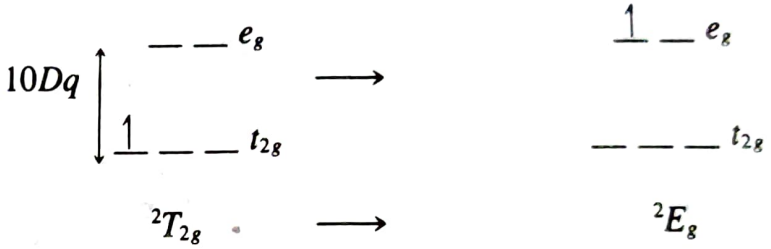

The right side of Figure 10.1 shows how the energy of each state changes as the field Dq increases. (This could be accomplished in principle by replacing the ligands with others lying successively higher in the spectrochemical series.) As the splitting between the states increases with the value of Dq, so does the energy of the transition between them. Thus, while the $^2T_{2g} \rightarrow {}^2E_g$ transition[3] occurs at 20,100 cm^{-1} for $[Ti(H_2O)_6]^{3+}$, it lies at 22,300 cm^{-1} for $[Ti(CN)_6]^{3-}$.

The absorption maximum for $[Ti(H_2O)_6]^{3+}$ in Figure 9.11 has a shoulder at about 17,400 cm^{-1} because of Jahn–Teller distortion (Section 9.8.2). This distortion splits the ^2E_g excited state to give $^2A_{1g}$ and $^2B_{1g}$. The distortion causes small splitting of the ground state ($^2T_{2g}$).

---

[2] The **magnetic dipole model** provides another mechanism for absorption of light by molecules in which the magnetic dipole oscillates when light is absorbed. Intensities for transitions in this model are orders of magnitude lower than those of electric-dipole-allowed transitions and have opposite selection rules—*they occur only with retention of parity* (i.e., $d \rightarrow d$ and $f \rightarrow f$ are allowed, but $p \rightarrow d$ is forbidden). Elements of the *f*-block absorb light according to this model, which we will not discuss further. Circular dichroism and optical rotatory dispersion involve the product of the integrals for electric dipole and magnetic dipole changes.

[3] Electronic spectroscopy began with atomic spectroscopy concerned with emissions from excited states to the ground state ex → gr. Early absorption spectroscopy used ex ← gr notation, but here we use gr → ex, as for $^2T_{2g} \rightarrow {}^2E_g$.

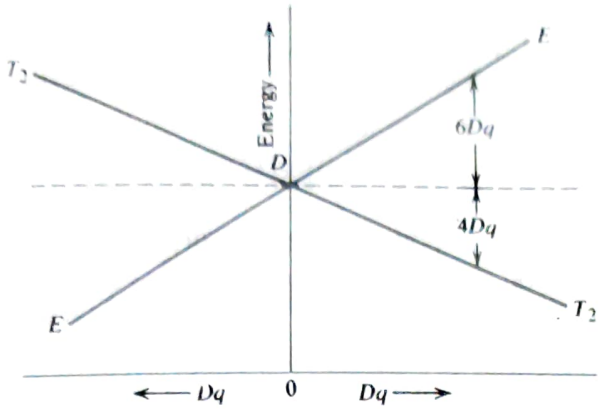

Figure 10.1 Orgel D term splitting diagram.

Because the splitting of the d orbitals is reversed for a tetrahedral field, so is the splitting diagram as shown on the left of Figure 10.1 with ^2E as the ground state.

We have seen that d^9 gives only one spectral term, ^2D—the electron can be missing from any one of the 10 possibilities. The transition in an octahedral field is $t_{2g}^6 e_g^3(^2E_g) \rightarrow t_{2g}^5 e_g^4(^2T_{2g})$—the "hole" has moved from e_g to the t_{2g} orbital set. A positive hole would be affected by the ligand field in just the opposite way as would a negative electron. This corresponds to a reversal of the sign of Dq and a ^2E_g ground state with a $^2T_{2g}$ excited state. The splitting diagram for octahedral d^9 is the reverse of d^1 (the left side of Figure 10.1). As before, the d^9 case for a tetrahedral complex is the reverse of that for an octahedron, or it corresponds to the d^1 octahedral case. In all these cases the transition energy is $10Dq$. The subscripts g and u are omitted from Figure 10.1 so that it applies to both $\mathbf{O_h}$ *and* $\mathbf{T_d}$ complexes.

The high-spin d^6 case gives only one quintet term ^5D, and this behaves like the d^1 case. We can consider that the half-filled configuration is unaltered and only the one electron of unique spin can move. Similarly, the high-spin d^4 case (also ^5D) corresponds to d^9—there is one "hole" in the half-filled d^5 configuration.

$$d^6 \quad \underline{\uparrow\downarrow}\ \underline{\uparrow}\ \underline{\uparrow}\ t_{2g} \qquad \underline{\uparrow}\ \underline{\uparrow}\ e_g$$

$$d^4 \quad \underline{\uparrow}\ \underline{\uparrow}\ \underline{\uparrow}\ t_{2g} \qquad \underline{\uparrow}\ \underline{\ }\ e_g$$

Thus, a single diagram (called an **Orgel diagram**) in Figure 10.1 shows the change in energy with Dq for four different configurations, all corresponding to one electron or one hole. It is qualitative because even for the same ligand $Dq_{oct} > Dq_{tet}$; besides, Dq depends on the particular metal ion. No spin multiplicities are shown for the states in Figure 10.1, so that the diagram applies to the four configurations discussed.

Configurations d^4 and d^6 give rise to many spectral terms other than D, but they differ in spin multiplicity. If we concentrate only on transitions which obey the spin-selection rule (the most intense ones), then also for high-spin d^4 and d^6 a single $d \rightarrow d$ band of ap-

preciable intensity is expected. The spectrum of the d^4 complex $[CrCl_6]^{4-}$ (present in $CrCl_2$ in molten $AlCl_3$ at 227°C and 5.6 atm) in Figure 10.2*a* shows the expected single absorption band with a maximum at 10,200 cm^{-1} with no apparent splitting. The spectrum of $[Fe(H_2O)_6]^{2+}$ (high-spin d^6) in Figure 10.2*b* shows a maximum at 10,400 cm^{-1} with a pronounced shoulder at 8300 cm^{-1}. The splitting results from Jahn–Teller distortion as for $[Ti(H_2O)_6]^{3+}$.

The spectra of Figures 9.11 and 10.2 show that light absorption occurs over a range of wavelengths. That is, complex ions do not give line spectra as are seen for gaseous atoms; instead we see *broad absorption bands*. This is so, even though the choice of a particular ligand would be expected to dictate a particular value of Dq and an exact energy of the transition corresponding to the distance between the state energies in the Orgel diagram. A major reason for the broad bands is that the value of Dq is very sensitive to the metal–ligand distance. Vibrations of the M—L bond change this distance and, in effect, sweep out a range of Dq values. These broad bands cover weak spin-forbidden transitions unless their peaks are isolated from other transitions.

One absorption band with the energy $10Dq$ is expected for d^9 with possible splitting of the band because of Jahn–Teller distortion. The only common d^9 ion is Cu^{2+}. The CuL_6^{2+} complexes such as $[Cu(NH_3)_6]^{2+}$ have large distortion with two long M—L bonds along z. This *tetragonal* distortion, $\mathbf{D_{4h}}$, is great enough to require the use of the lower ($\mathbf{D_{4h}}$) symmetry rather than $\mathbf{O_h}$ for interpretation of the spectra. In addition, spin–orbit coupling is significant for copper, and this causes additional splitting of energies.

Splittings for d^2, d^3, d^8, and High-Spin d^7

The d^2 case is the simplest one where we deal with both (a) the splitting of orbital degeneracy and (b) the effect of electron repulsion.[4] The d^2 configuration has two terms of maximum spin-multiplicity for the free ion: ^3F (the ground state) and ^3P. These differ in energy by $15B$.[5] As Table 10.1 shows, ^3P gives $^3T_{1g}$ and the ground state ^3F term splits in an octahedral field into $^3T_{1g} + {}^3T_{2g} + {}^3A_{2g}$. The relative energies of these states can be calculated by techniques beyond the scope of this book and are given in Figure 10.3*a*. Note that the zero of energy is the ground-state energy of the ^3F term of the free ion obtained from atomic spectroscopy. The ^3P term (as for p orbitals) does not split and becomes $^3T_{1g}$ in $\mathbf{O_h}$. The diagram shows how the state energies change with Dq.

The two $^3T_{1g}$ states in Figure 10.3 are distinguished by their "parentage" in parentheses: $^3T_{1g}(F)$ and $^3T_{1g}(P)$. Because they have the same symmetry properties in an octahedral field, these two states can interact with each other. As Dq_{oct} increases, the wavefunc-

[4] To be sure, electron repulsion is present for the 4-, 6-, and 9-d-electron cases. However, the high-spin cases all correspond to the motion of just one electron among the manifold of split d orbitals while the rest of the electrons remain in a fixed configuration. Thus, as long as we confine ourselves to cases where no spin changes occur (the spin-allowed transitions), the electron repulsion does not change in any of the transitions and thus does not contribute to their energies. In contrast, two d electrons can adopt a variety of orbital arrangements, all corresponding to triplet spin states.

[5] The energy separations of spectroscopic terms are expressed in terms of Racah parameters B and C. For terms of maximum spin multiplicity, this separation is only a function of B. B and C are different for each atom or ion and are evaluated from atomic spectra. The value of B, labeled as B', is lower in complexes because of electron delocalization.

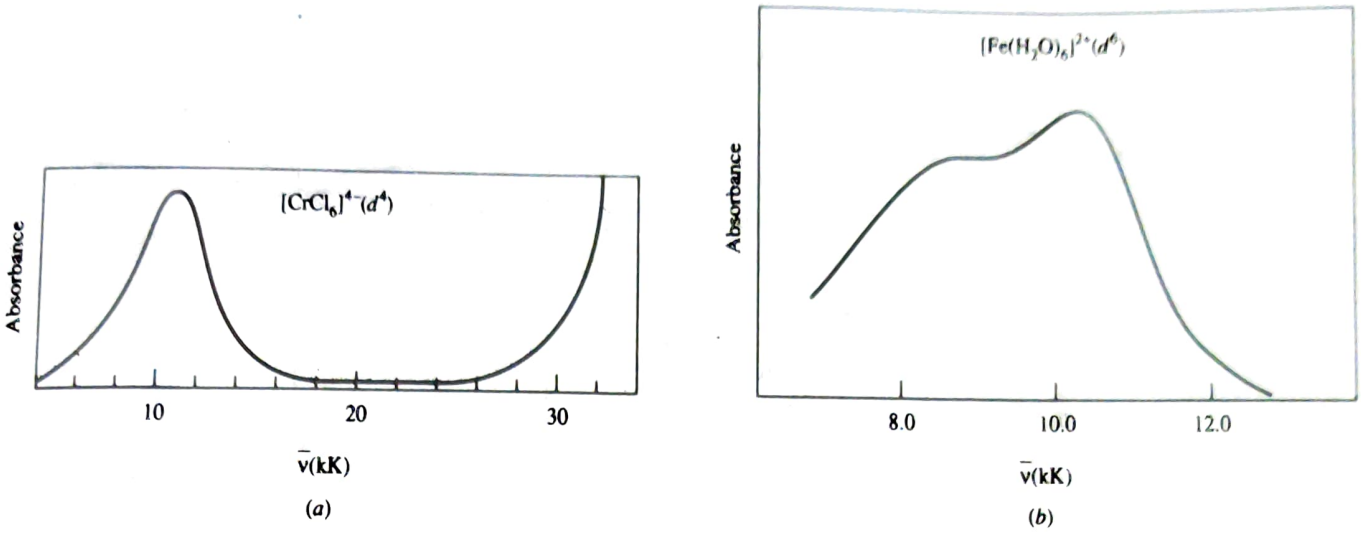

Figure 10.2 (*a*) Absorption spectrum of $[CrCl_6]^{4-}$ using $CrCl_2$ in $AlCl_3$ at 227°C and 5.6 atm. (Adapted with permission from H. A. Øye and D. M. Gruen, *Inorg. Chem.* **1964**, *3*, 836. Copyright 1964 American Chemical Society.) (*b*) Absorption spectrum of $[Fe(H_2O)_6]^{2+}$.

tion of the $^3T_{1g}(F)$ ground state mixes in increasing amounts of the $^3T_{1g}(P)$ wavefunction, and vice versa. (We say that mixing of the states, or configuration interaction, occurs.) The result is that the energies of these two states deviate from what their values would have been in the absence of interaction, bending away from each other instead of displaying the linear behavior (dashed lines) otherwise expected as shown in Figure 10.3*b*. This is referred to as the **noncrossing rule.**[6]

In an extremely weak O_h field (so weak that no curvature of the $^3T_{1g}$ states yet occurs), a d^2 complex is expected to display three transitions from the $^3T_{1g}(F)$ ground state to: $^3T_{2g}(\nu_1 = 6Dq + 2Dq = 8Dq)$, $^3A_{2g}(\nu_2 = 18Dq)$, and $^3T_{1g}(P)(\nu_3 = 6Dq + 15B)$, as shown in Figure 10.3*a*. For a stronger field (after curvature has set in) the energies of all the transitions will be increased by the amount that the ground-state energy has been lowered due to curvature. Band ν_3 will increase by the additional amount corresponding to the raising of the $^3T_{1g}(P)$ energy. At still higher values of Dq, the $^3T_{1g}(F) \rightarrow {}^3T_{1g}(P)$ transition is at lower energy than $^3T_{1g}(F) \rightarrow {}^3A_{2g}$.

For d^8, the two-hole case, holes are affected in the opposite way when compared to two electrons (Dq is reversed in sign), and we can extrapolate the straight lines to the left in Figure 10.3*b*. Here the ground state is $^3A_{2g}$. The noncrossing rule still applies, and the lines for the $^3T_1$ states bend away from each other. The resulting curvature is greater than for d^2 because the energies of the unperturbed states are closer and must not cross. Now because of bending, the energy for $^3A_2 \rightarrow {}^3T_1(F)$ is *less* than $18Dq$ and that of $^3A_2 \rightarrow {}^3T_1(P)$ is *greater* than $12Dq + 15B$. The hole formalism relates the configurations d^8 to d^2

[6] We have already seen in Chapter 4 that only orbitals with the same symmetry properties can interact to form molecular orbitals (MOs). This is also true of the many-electron wavefunctions (states) which are required by quantum mechanics to interact if their symmetry behavior is the same. Just as mixing of orbitals to form MOs is greater when the orbitals are of similar energies, so is the mixing of states more extensive as the unperturbed states approach more closely in energy; thus, the curvature of the plot increases for both the lower and upper states. See R. W. Jotham, *J. Chem. Educ.* **1975**, *52*, 377.

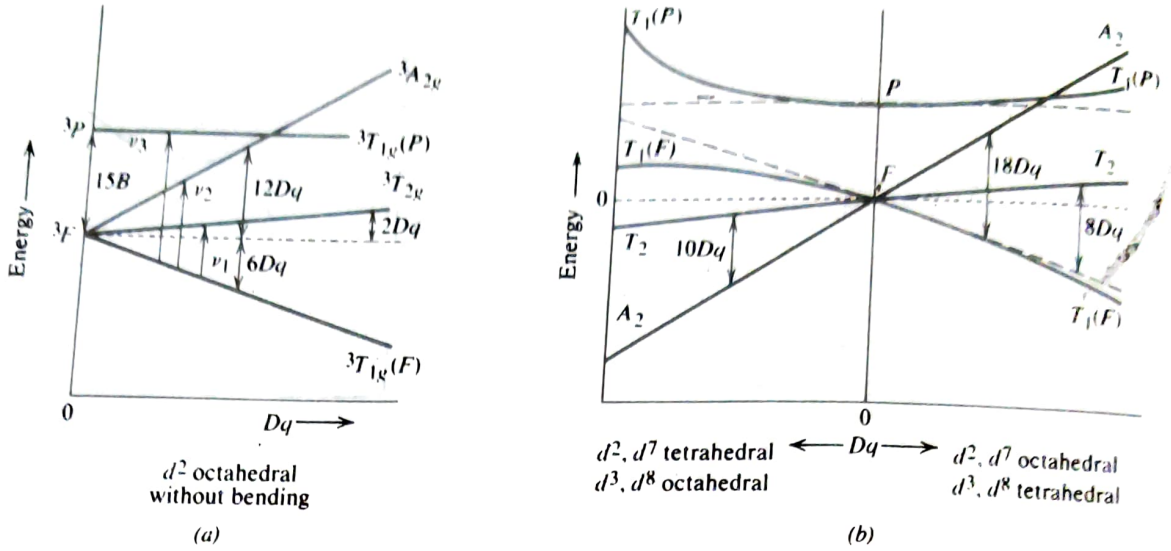

Figure 10.3 Orgel term splitting diagram for d^2, d^3, d^7, and d^8 cases in octahedral and tetrahedral fields. (Adapted with permission from L. E. Orgel, *J. Chem. Phys.* **1955**, *23*, 1004.)

and d^3 to high-spin d^7 as shown in the diagram. Figure 10.4 shows the effect of splitting and curving from state mixing for transitions for d^3 and d^8 in an octahedral field. The energies of the transitions for d^3 and d^8 ($\mathbf{O}_h$) with c for the bending are

$$\begin{aligned} \nu_1 &= 10Dq \\ \nu_2 &= 18Dq - c \\ \nu_3 &= 15B' + 12Dq + c \end{aligned} \tag{10.7}$$

EXAMPLE 10.2: $[Cr(H_2O)_6]^{3+}$ shows three absorption bands at 17.4, 24.6, and 37.9 kK. Assign the three bands and calculate Dq, c, and B'.

Solution:

$$\nu_1 = 10Dq = 17.4 \text{ kK} \quad \text{or} \quad Dq = 1.74 \text{ kK}$$

$$\nu_2 = 18Dq - c = 18(1.74) - c = 24.6 \quad \text{and} \quad c = 6.7 \text{ kK}$$

$$\nu_3 = 15B' + 12Dq + c = 37.9$$

$$15B' = 37.9 - 20.9 - 6.7 = 10.3, \qquad B' = 0.69 \text{ kK}$$

B for Cr^{III} is 1.06 kK for the free ion.

Summary for High-Spin d^n Ions

Only two diagrams (Figures 10.1 and 10.3) are needed to describe the splitting of terms of maximum spin multiplicity for all configurations, except d^5, because they all have D or F ground-state terms. The d^5 configuration is unique. It is its own hole counterpart and there are no spin-allowed transitions; there is only one sextet, the ground-state $^6A_{1g}$. Octahedral high-spin d^5 ions (e.g., $[Mn(H_2O)_6]^{2+}$) are faintly colored because all $d \rightarrow d$ transitions are spin-forbidden. However, because there are several ways to arrange four electrons of one spin set and one of the other spin set, there are four free-ion quartet terms and many quartet states arise in an octahedral field, leading to many peaks of very low intensity. This spectrum will be discussed on page 455.

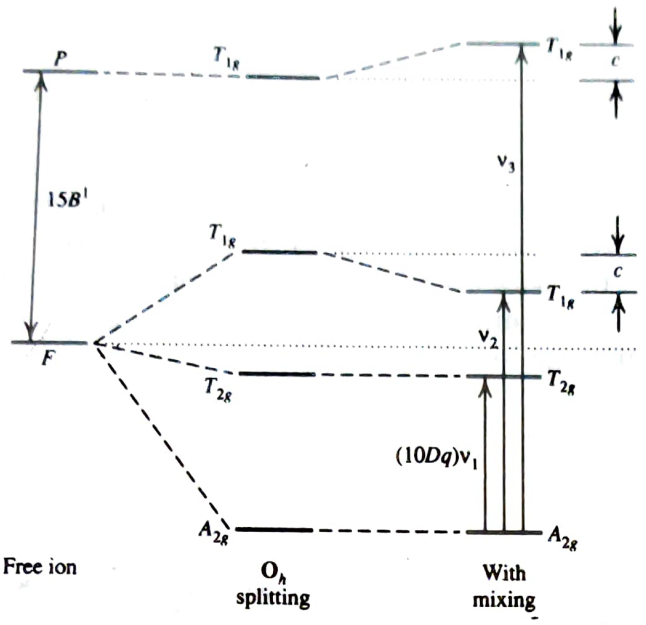

Figure 10.4 Splitting and mixing of states for d^3 and d^8 ions in an octahedral field, for a single value of Dq.

A single absorption band is expected for octahedral complexes of d^1 and d^9, as well as high-spin d^4 and d^6 ions. The band might be unsymmetrical or split because of Jahn–Teller splitting of the e_g level whether these orbitals are occupied unequally in the ground state (d^4 and d^9) or in the excited state (d^1 and d^6). The splitting is greater for e_g than for t_{2g} occupancy (see Section 9.8.2). Octahedral complexes of ions with the other high-spin configurations (except d^5) are expected to show three ligand-field absorption bands.[7] The energies of two of the transitions [to $T_{1g}(P)$ and A_{2g}] are nearly the same in fields of intermediate strength (near where these lines in Figure 10.3 cross), and they might appear as a single broad band.

Orgel diagrams apply only to high-spin complexes. They describe what happens to energies of states starting from the free ions (where only electron repulsion energies are significant) as orbital energies split because the ligand field increases from zero to a magnitude comparable to that of the electron-repulsion energy. In the range of applicability of Orgel diagrams, both these energy contributions determine the placement of electrons. If Dq were increased sufficiently, the orbital-splitting energies would ultimately become much greater than the electron repulsion energies and would be the major factor determining electron placement. As we saw in Section 9.8.1, this leads to low-spin complexes with change in spin multiplicity of the ground state. In Section 10.2.5 we will examine how to deal with this case where $10Dq >>$ electron repulsion energy.

EXAMPLE 10.3: What are the lowest energy transitions for high-spin octahedral ML_6^{n+} complexes for V^{3+}, Cr^{3+}, Mn^{2+}, Ni^{2+}, and Cu^{2+}?

Solution: Using Figures 10.1 and 10.3, we obtain

$$V^{3+}\ d^2\text{:}\ {}^3T_{1g} \longrightarrow {}^3T_{2g} \qquad Ni^{2+}\ d^8\text{:}\ {}^3A_{2g} \longrightarrow {}^3T_{2g}$$

$$Cr^{3+}\ d^3\text{:}\ {}^4A_{2g} \longrightarrow {}^4T_{2g} \qquad Cu^{2+}\ d^9\text{:}\ {}^2E_g \longrightarrow {}^2T_{2g}$$

$$Mn^{3+}\ d^4\text{:}\ {}^5E_g \longrightarrow {}^5T_{2g}$$

[7] Ligand-field bands are those involving $d \rightarrow d$ transitions.

▸ 10.2.4 *The Spectrum of $[CoF_6]^{4-}$*

An example of the splitting of states described above is seen in the absorption spectrum of crystals of $KCoF_3$ in which $Co^{2+}(d^7)$ is surrounded octahedrally by $6F^-$. Absorption bands centered at 7.15, 15.2, and 19.2 kK (1kK = 1000 cm^{-1}) are seen in Figure 10.5. For a weak-field ligand such as F^- we expect from Figure 10.3 that these bands should correspond to $^4T_{1g} \rightarrow {}^4T_{2g}$, $^4T_{1g} \rightarrow {}^4A_{2g}$, and $^4T_{1g} \rightarrow {}^4T_{1g}(P)$, respectively. We could calculate Dq from ν_1, which is $8Dq$, but this does not allow for configuration interaction (bending) between the T_{1g} states. The $(\nu_2 - \nu_1)$ difference is $10Dq$ $(18Dq - 8Dq)$ giving $10Dq$ = 15.2 − 7.2 = 8.0 kK. From the expressions

$$\nu_1 = 8Dq + c \tag{10.8}$$

$$\nu_2 = 18Dq + c \tag{10.9}$$

(where c is the bending from configuration interaction), we get c = 0.8 kK in each case. We see from Equations (10.8) and (10.9) that c cancels for $\nu_2 - \nu_1$.

The Racah parameter B for the complex can be evaluated from ν_3; the value of B in complexes (B') is always less than the value for the free ion.

$$\nu_3 = 15B' + 6Dq + 2c \tag{10.10}$$

This gives B' = 0.85 kK, compared with the free-ion value for Co^{2+} of 0.97 kK. Typically, $B' = 0.7B$ to $0.9B$ because of the decreased electron repulsion caused by greater delocalization of the d electrons in the complex. Jørgensen calls this decreased repulsion the **nephelauxetic** ("cloud expanding") **effect.** It arises because the actual bonding in the complexes departs from the crystal field model in which the only function of ligands is to provide an electric field of particular symmetry. Actually, ligand electrons interact with the central metal atom in two ways: First, the electrons of the ligand partly invade the space of the metal electrons, thus partially screening the metal nuclear charge from its

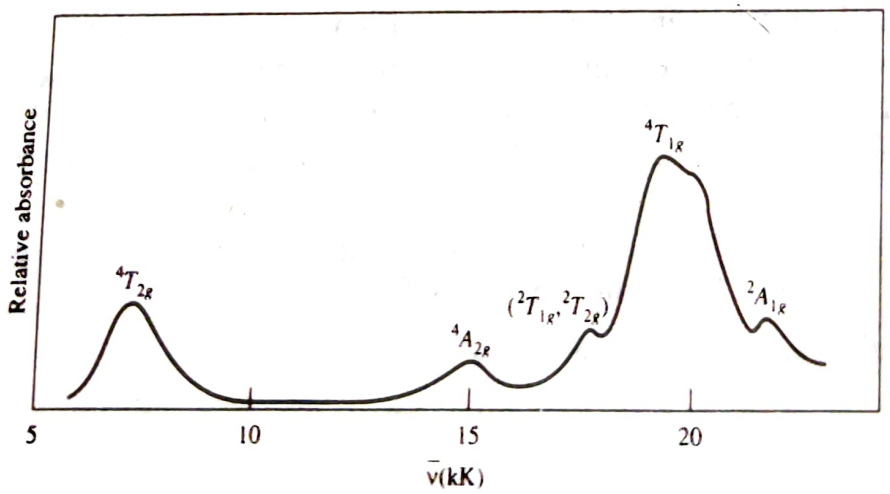

Figure 10.5 The absorption spectrum of $[CoF_6]^{4-}$ in a crystal of $KCoF_3$ at 150 K. (Adapted from J. Ferguson, D. L. Wood, and K. Knox, *J. Chem. Phys.* **1963**, *39*, 881.)

own electrons. Because the electrons are then less tightly held, the electron cloud expands and interelectronic repulsion is reduced. Second, MO formation between metal and ligand orbitals occurs. (This is treated in detail in Section 10.6.) For now, we note that the contribution of ligand orbitals to occupied MOs can lead to the delocalization of metal electrons onto the ligand, further reducing electron repulsion. We obtain values of B' empirically from spectra, and for a given metal the ratio B'/B decreases roughly as follows[8]:

$$F^- > H_2O > NH_3 > en > NCS^- > Cl^- \sim CN^- > Br^- > S^{2-} > I^-$$

This ranking is referred to as the **nephelauxetic series.** The value of B' for $[CoF_6]^{4-}$ is $0.85B$, indicating the small amount of interaction between F^- and Co^{2+} electrons. If we do not know the value of B', we can use $\sim 0.8B$ as a reasonable approximation.

The example of $[CoF_6]^{4-}$ is for a crystal of $KCoF_3$, and the spectrum of $[CrCl_6]^{4-}$ (Figure 10.2) is for $CrCl_2$ in molten $AlCl_3$. These examples are used because well-defined species are present. In solution, many complexes of Co^{III} and Cr^{III} are stable with respect to substitution by other ligands—the complexes are called **inert** (substitution-inert). We can get stable geometrical and optical isomers of these complexes. For complexes of many other metal ions, substitution of one ligand by another occurs readily—these complexes are ~~called~~ **labile.** In these cases there can be equilibria among several species in solution, depending upon concentrations. Species such as $[CoF_6]^{4-}$ and $[CrCl_6]^{4-}$ cannot be identified in aqueous solution.
